Spintronic Materials

International Edition: DOI: 10.1002/anie.201503824
German Edition: DOI: 10.1002/ange.201503824

Unconventional Magnetic and Resistive Hysteresis in an Iodine-Bonded Molecular Conductor**

Genta Kawaguchi, Mitsuhiko Maesato, Tokutaro Komatsu, Hiroshi Kitagawa, Tatsuro Imakubo, Andhika Kiswandhi, David Graf, and James S. Brooks†*

In memory of James S. Brooks

Abstract: *Simultaneous manipulation of both spin and charge is a crucial issue in magnetic conductors. We report on a strong correlation between magnetism and conductivity in the iodine-bonded molecular conductor $(DIETSe)_2FeBr_2Cl_2$ [DIETSe = diiodo(ethylenedithio)tetraselenafulvalene], which is the first molecular conductor showing a large hysteresis in both magnetic moment and magnetoresistance associated with a spin-flop transition. Utilizing a mixed-anion approach and iodine bonding interactions, we tailored a molecular conductor with random exchange interactions exhibiting unforeseen physical properties.*

The discovery of giant magnetoresistance (GMR) in alternating ferromagnetic and nonmagnetic metal layers[1] has opened the field of spintronics.[2] Compared to the top-down approach in inorganics, molecular materials have advantages in bottom-up and low-cost fabrication as well as diverse material design. Although molecular materials normally show weak interactions, when competing interactions are delicately balanced, small perturbations can give rise to a giant response.[3] Some π–d hybrid molecular conductors indeed show interesting spin-charge-coupled phenomena,[4] such as GMR[4a] and field-induced superconductivity.[4b]

Multi-instability or switching function is also an important issue in magnetic conductors. Quasi-one-dimensional (Q1D) π–d conductors[5–8] are good candidates having such properties because Q1D metals are susceptible to external stimuli due to low-dimensional instability. Recently, we found spin-flop switching and memory in $(DIETSe)_2FeCl_4$, where DIETSe denotes diiodo(ethylenedithio)tetraselenafulvalene (Figure 1 a).[7] However, the hysteresis was only observed in resistance.

To introduce large hysteresis in both magnetism and conductivity, we propose to use a mixed-anion material, in which magnetic anions are mixed in a radical cation salt to induce random exchange interaction.

Herein we report on the discovery of large hysteresis in both magnetism and magnetoresistance (MR) associated with a spin-flop transition in a mixed-anion π–d conductor $(DIETSe)_2FeBr_2Cl_2$ (**1**). In contrast to inorganics, molecular

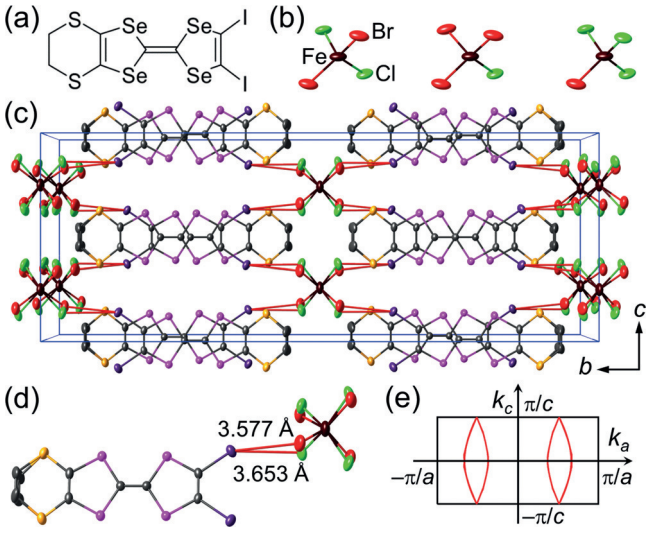

Figure 1. a) Molecular structure of DIETSe. b) Anions in a crystal of **1**. c) Crystal structure of **1** viewed along the *a*-axis. C: gray, I: violet, Se: pink, S: yellow, Fe: brown, Br: red, and Cl: green. Thermal ellipsoids represent 50% probability. The site occupancy factors of Br and Cl are 0.5. Red lines show iodine bonds. d) Short contacts due to iodine bonds. e) Fermi surfaces of **1** in the k_c–k_a plane.

[*] G. Kawaguchi, Prof. Dr. M. Maesato, Dr. T. Komatsu, Prof. Dr. H. Kitagawa
Division of Chemistry, Graduate School of Science
Kyoto University, Sakyo-ku, Kyoto 606-8502 (Japan)
E-mail: maesato@kuchem.kyoto-u.ac.jp
Prof. Dr. H. Kitagawa
JST-CREST
Goban-cho 7, Chiyoda-ku, Tokyo 102-0075 (Japan)
Prof. Dr. T. Imakubo
Department of Materials Science and Technology
Nagaoka University of Technology
1603-1 Kamitomioka, Nagaoka, Niigata 940-2188 (Japan)
Dr. A. Kiswandhi,[+] Dr. D. Graf, Prof. Dr. J. S. Brooks
National High Magnetic Field Laboratory
Florida State University
1800 E. Paul Dirac Dr., Tallahassee, FL 32310-3706 (USA)
[+] Present address: Department of Physics, University of Texas at Dallas, Richardson (USA)
[†] Deceased on September 27, 2014.

[**] The work was supported in part by Grants-in-Aid for JSPS Fellows (25-1778), Scientific Research (C) (25400367), (C) (25410090), (S) (23225005) from JSPS, and NSF-DMR 1157490, 1309146, the State of Florida, and the US DOE. The calculations and modellings were performed on the supercomputer of ACCMS, Kyoto University and SuperComputer System, Institute for Chemical Research, Kyoto University.

Supporting information for this article is available on the WWW under http://dx.doi.org/10.1002/anie.201503824.

materials have difficulties in alloying or chemical doping, while maintaining its crystal structure. It is because of weak intermolecular interactions, such as van der Waals interaction. By using iodine bonds,[6,9] however, we succeeded in fabricating the isostructural mixed-anion salts. This method allowed us to fine-tune π–d interactions and low-dimensional instability of itinerant π-electrons in Q1D π–d systems.

The DIETSe molecule was synthesized as described in the literature.[10] Single crystals of **1** and $(DIETSe)_2GaBr_2Cl_2$ (**2**) were prepared by an electrolytic method using supporting electrolytes of equimolar TBA–MBr_4 and TBA–MCl_4 [TBA = tetra-*n*-butylammonium; M = Fe, Ga]. The Br/Cl ratio was confirmed to be the same with synthetic ratio from energy-dispersive X-ray (EDX) analysis (Table S1 in the Supporting Information (SI)). We note that, as shown in Figure 1 b, several halogen-mixed anion species $MBr_xCl_{4-x}^-$ [M = Fe, Ga; $x = 0$, 1, 2, 3, 4] with majority of averaged-formula species are considered to coexist in a crystal with random orientation because such coexistence has been observed in $GaCl_4^-/GaBr_4^-$ mixture solution by ^{71}Ga nuclear magnetic resonance (NMR) study.[11]

The crystal structures of **1** and **2** are isostructural to the pristine $(DIETSe)_2MX_4$ [M = Fe, Ga; X = Br, Cl] (Figure 1 c; Figures S1 and S2).[6,12] DIETSe molecules uniformly stack parallel to the *a*-axis in a head-to-tail manner, giving rise to the highest conductivity along the *a*-axis direction. Figure 1 d shows short I···X [X = Br, Cl] contacts between DIETSe and anion, which are shorter than the sum of the van der Waals radii: I···Cl = 3.73 Å, I···Br = 3.83 Å, indicating that the iodine bonds play an important role in stabilizing the structure.[6,9] The MBr_2Cl_2 [M = Fe, Ga] salts have nearly the same lattice parameters (Table S2). The Ga^{3+} ion is nonmagnetic ($S = 0$), while the Fe^{3+} ion has localized d-spins ($S = 5/2$). Therefore, **2** is a good reference with which to extract the nature of itinerant π-electrons. The band structures and Fermi surfaces of **1** and **2** were calculated based on the density-functional theory (Figure 1 e, details in SI), indicating a Q1D electronic structure.

The temperature-dependent resistivities of **1** and the pristine FeX_4 [X = Br, Cl] salts are shown in Figure 2 a. As shown by dashed arrows, the $FeCl_4$ salt and **1** undergo a metal–insulator (M–I) transition at 11 and 8 K, respectively. The similar M–I transition occurs in the $GaCl_4$ salt and **2** at 12 and 9 K, respectively (Figure S3). These are attributed to a spin density wave (SDW) transition from nesting instability of the Q1D Fermi surfaces. The previous ^{77}Se NMR study has confirmed an incommensurate SDW formation in the $GaCl_4$ salt.[13] In contrast, the $GaBr_4$ salt is metallic down to 1.9 K (Figure S3). These results indicate Br substitution suppresses the SDW transition to lower temperatures owing to an increase in the warping of Fermi surfaces. Besides the SDW transition, an additional steep increase in the resistivity, which is absent in the nonmagnetic Ga salts, appears at 2.5, 4, and 7 K in the $FeCl_4$ salt, **1**, and $FeBr_4$ salt, respectively (solid arrows). These anomalies correspond to antiferromagnetic (AF) transitions of d-spins, as discussed below.[6,7] The Néel temperature T_N increases with Br content, indicating systematic control of π–d interactions by anion mixing.

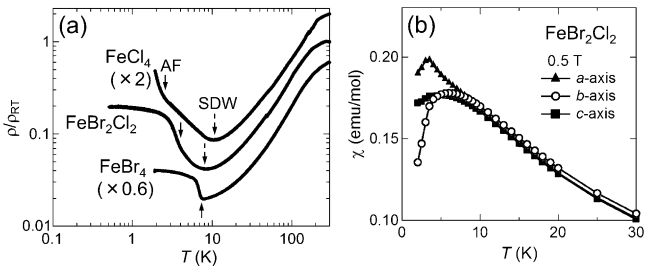

Figure 2. a) Electrical resistivity along the *b*-axis of the $FeCl_4$ salt, **1**, and $FeBr_4$ salt, normalized by the value at 300 K. For clarity, the values of the $FeCl_4$ and $FeBr_4$ salts are multiplied by 2 and 0.6, respectively. Broken and solid arrows show SDW and AF transitions, respectively. b) Magnetic susceptibility of **1** at 0.5 T along the *a*- (filled triangles), *b*- (open circles), and *c*-axes (filled squares).

Figure 2 b and Figure S4 show the temperature dependence of the magnetic susceptibility χ of **1** along each crystallographic axis. Above 20 K, χ is well fitted by the Curie–Weiss law with Curie constant $C = 4.5$ emu K mol^{-1} and Weiss temperature $\theta = -14$ K (Figure S4). Below 4 K, χ decreases with lowering temperature in an anisotropic nature, indicating long-range AF ordering with a magnetic easy axis along the *b*-axis. Since the value of $T_N = 4$ K agrees well with the resistivity anomaly (Figure 2 a), the steep increase in resistance at T_N implies an AF ordering-induced charge gap. Assuming that the up- and down-spins of Fe^{3+} alternately order along the *a*-axis by an AF transition, $2k_F$ ($= \pi/a$) periodic modulation of the local moments appears, which can induce charge gap opening via strong π–d interactions.

To explore the magnetic-field effects on the electronic states, we employed a magnetic torque technique (details in SI). Figure 3 a shows the magnetic torque τ divided by the field strength up to 35 T along the *b*-axis. Below 2 K, a sharp increase in τ/H appears around 2 T, attributed to spin-flop transitions of d-spins. Anomalies are also observed around 7 T below T_N, indicating AF boundaries, which are plotted as filled diamonds in the temperature–magnetic field (T–H) phase diagram (Figure 4). In addition, τ/H shows a maximum above 15 T, and with increasing temperature, it shifts to higher fields, suggesting the saturation field H_{FM} (filled squares in Figure 4). This is also supported by the magnetization M measured at 2 K using a superconducting quantum interference device (SQUID) magnetometer: the linear extrapolation of M reaches 5 μ_B at about 13 T, which is comparable to H_{FM} (15 T) (Figure 3 a). The obtained H_{FM} is almost intermediate between that of the $FeCl_4$ (6 T)[7] and $FeBr_4$ salts (22 T; also see Figure S5).[8] A wide gap is observed between the AF boundary and saturation field in **1**. This indicates no long-range order but a short-range order or fluctuations in the intermediate paramagnetic (PM) region, which is pronounced by anion mixing.

We discovered unconventional magnetic hysteresis at very low temperatures (< 1 K) by SQUID with a ^{3}He cryostat. Figure 3 b displays a clear large hysteresis in magnetization M at 0.5 K, associated with a spin-flop transition (also see Figure S6). We also observed a similar hysteresis in magnetic torque at 0.3 K (Figure S5). The down-sweep magnetization, M_{down}, is significantly larger than the up-sweep one, M_{up}

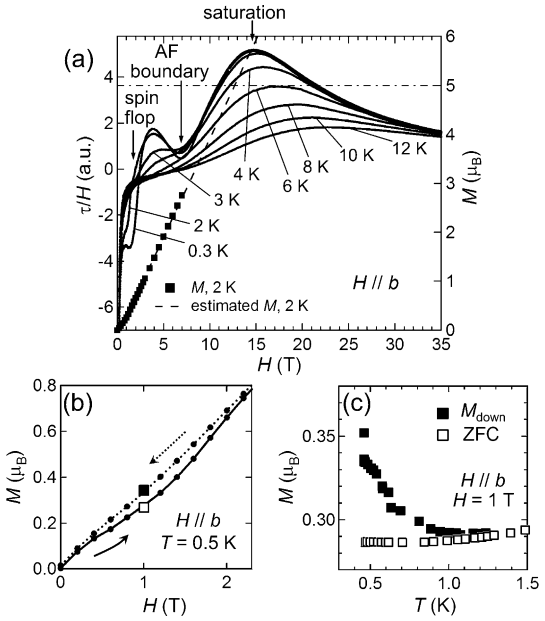

Figure 3. Magnetic torque and magnetization of **1** under magnetic field along the *b*-axis. a) Magnetic field dependence of torque divided by magnetic field, τ/H (left axis) and extrapolated magnetization (right axis). b) Magnetic field dependence of magnetization *M* at 0.5 K. Solid and dotted curves indicate *M* for up- and down-sweeps, respectively. c) Temperature dependence of *M* at 1 T. Open and filled squares denote ZFC and M_{down}, heating after field sweeping up to 5 T, respectively. Enlarged open and filled squares in (b) correspond to the initial points of ZFC and M_{down} in (c), respectively.

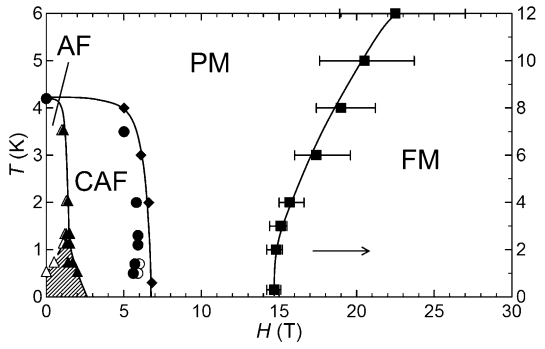

Figure 4. Temperature–magnetic field phase diagram of **1**. AF: antiferromagnetic, CAF: canted AF, PM: paramagnetic, FM: ferromagnetic. Filled diamonds show magnetic torque minimum. Filled squares represent maximum of torque (right axis). Filled and open triangles represent dip structures in up- and down-sweep magnetoresistance (MR, see Figure 5), respectively. Filled and open circles denote up- and down-sweep MR minimum, respectively. The shaded region shows hysteresis.

(Figure 3b). The field-induced state is found to be metastable, and the hysteresis disappears on subsequent heating. Figure 3c shows the temperature dependence of *M* at 1 T for the zero field cooled (ZFC) (open squares) and M_{down} (filled squares) after the field sweep at 0.5 K, whose initial points are equivalent to the emphasized squares in Figure 3b (also see SI). M_{down} decreases with increasing temperature and follows ZFC above 1.3 K, which is well reproduced by two different samples (Figure S7). These results indicate the hysteresis emerges only below 1.3 K.

Remarkably, the anomalous hysteresis also appears in the resistivity. Figure 5 shows MR of **1** under the magnetic field along the *b*-axis. Below T_N (4 K), the MR shows large anomalies with hysteresis, in sharp contrast to the monotonic

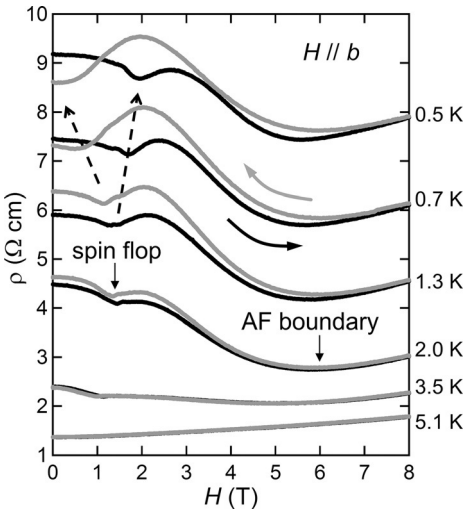

Figure 5. Magnetoresistance (MR) of **1** under the magnetic field along the *b*-axis. The data for 1.3, 0.7, and 0.5 K are shifted upward for clarity. Up- and down-sweep MR are shown in black and gray, respectively.

MR in **2** (Figure S8). The former clearly demonstrates significant π–d interactions between itinerant π-electrons and AF d-spins. The dip structure in MR at 1.4 T and 2 K is attributed to a spin-flop transition of d-spins, which is confirmed by magnetic torque and magnetization (Figure S9). Furthermore, below 1.3 K the dip position shifts to higher and lower fields for up- and down-sweeps, respectively, as indicated by the broken arrows in Figure 5 and filled (up-sweep) and open (down-sweep) triangles in *T*–*H* phase diagram (Figure 4). The shaded region in Figure 4 is in good accordance with the magnetic hysteresis. In fact, the low-temperature hysteretic behaviors of MR, magnetization, and magnetic torque are well correlated (Figure S10). At higher magnetic fields, a negative MR is observed. As denoted by filled (up-sweep) and open (down-sweep) circles in *T*–*H* phase diagram (Figure 4), the broad minimum in MR around 6 T corresponds to the AF boundary, in good agreement with the torque results.

The large hysteresis in *M* and the cusp in χ along the *a*-axis at T_N (Figure 2b) are reminiscent of weak ferromagnetism from spin canting.[14] However, the hysteresis is negligible near to zero field, in contrast to typical canted AF (CAF) systems.[15] Instead, *M* shows a large hysteresis around the spin-flop field (Figure 3b). Spin flop is a first-order transition, and therefore, involves hysteresis. However, the hysteresis is normally very small, as seen in the pristine FeX_4 [X = Br, Cl] salts (Figure S5). On the other hand, **1** shows an extraordinarily large hysteresis around spin-flop field below 1.3 K. These results suggest that anion mixing plays a key role in the

hysteresis phenomena. The randomly substituted halide ions (Cl or Br) induce random magnetic interactions. The so-called random exchange effect can in part account for the enhancement of the hysteresis at spin-flop field, as discussed for some inorganic alloys.[16] The less pronounced spin-flop transition in down-sweep *M* implies continuous changes in the domain ratio of coexisting AF and CAF phases. In contrast to a homogeneous system, a number of pinning centers may be present in the mixed halide system, giving rise to a significant effect on the domain wall dynamics.

The spin and charge degrees of freedom are strongly coupled with each other in **1**. The coexistence of AF ordering of d-spins and SDW of π-electrons, and their interplay would be essential for the peculiar magnetic and transport properties. It is known that density waves become glassy at low temperatures.[17] We also note that the hysteresis is significantly pronounced only below 1.3 K. A synergistic effect between the glassy nature of SDW and the random exchange is a possible origin for the unconventional hysteresis.

In conclusion, we successfully synthesized mixed-anion π–d conductor **1** while keeping the isostructure utilizing iodine bonds. Compound **1** is the first example of a molecular conductor showing a large hysteresis associated with a spin-flop transition in both magnetization and conductivity via strong π–d interactions. We also succeeded in tuning the SDW instability and π–d interactions by anion mixing. Our results suggest that chemical substitution can cause systematic and drastic changes in the electronic states, and that iodine-bonded supramolecular systems can be useful to obtain strong correlations. We believe our study will open up the potential of novel physical phenomena and multifunctionality for electronics and spintronics.

Keywords: conducting materials · iodine · magnetic properties · organic–inorganic hybrid composites · random exchange interaction

How to cite: *Angew. Chem. Int. Ed.* **2015**, *54*, 10169–10172
Angew. Chem. **2015**, *127*, 10307–10310

[1] a) M. N. Baibich, J. M. Broto, A. Fert, F. Nguyen Van Dau, F. Petroff, P. Etienne, G. Creuzet, A. Friederich, J. Chazelas, *Phys. Rev. Lett.* **1988**, *61*, 2472–2475; b) G. Binasch, P. Grünberg, F. Saurenbach, W. Zinn, *Phys. Rev. B* **1989**, *39*, 4828–4830.

[2] a) S. A. Wolf, D. D. Awschalom, R. A. Buhrman, J. M. Daughton, S. von Molnár, M. L. Roukes, A. Y. Chtchelkanova, D. M. Treger, *Science* **2001**, *294*, 1488–1495; b) D. D. Awschalom, M. E. Flatté, *Nat. Phys.* **2007**, *3*, 153–159.

[3] a) M. Chollet, L. Guerin, N. Uchida, S. Fukaya, H. Shimoda, T. Ishikawa, K. Matsuda, T. Hasegawa, A. Ota, H. Yamochi, G. Saito, R. Tazaki, S. Adachi, S. Koshihara, *Science* **2005**, *307*, 86–89; b) F. Sawano, I. Terasaki, H. Mori, T. Mori, M. Watanabe, N. Ikeda, Y. Nogami, Y. Noda, *Nature* **2005**, *437*, 522–524.

[4] a) N. Hanasaki, H. Tajima, M. Matsuda, T. Naito, T. Inabe, *Phys. Rev. B* **2000**, *62*, 5839–5842; b) S. Uji, H. Shinagawa, T. Terashima, T. Yakabe, Y. Terai, M. Tokumoto, A. Kobayashi, H. Tanaka, H. Kobayashi, *Nature* **2001**, *410*, 908–910; c) E. Coronado, J. R. Galán-Mascarós, C. J. Gómez-García, V. N. Laukhin, *Nature* **2000**, *408*, 447–449; d) M. Kurmoo, A. W. Graham, P. Day, S. J. Coles, M. B. Hursthouse, J. L. Caulfield, J. Singleton, F. L. Pratt, W. Hayes, L. Ducasse, P. Guionneaul, *J. Am. Chem. Soc.* **1995**, *117*, 12209–12217; e) H. Kobayashi, H.-B. Cui, A. Kobayashi, *Chem. Rev.* **2004**, *104*, 5265–5288; f) T. Enoki, A. Miyazaki, *Chem. Rev.* **2004**, *104*, 5449–5477; g) *Multifunctional Conducting Molecular Materials* (Eds.: G. Saito, F. Wudl, R. C. Haddon, K. Tanigaki, T. Enoki, H. E. Katz, M. Maesato), RSC Publishing, Cambridge, **2007**; h) *Multifunctional Molecular Materials* (Ed.: L. Ouahab), Pan Stanford, Singapore, **2013**.

[5] a) K. Enomoto, J. Yamaura, A. Miyazaki, T. Enoki, *Bull. Chem. Soc. Jpn.* **2003**, *76*, 945–959; b) K. Okabe, J. Yamaura, A. Miyazaki, T. Enoki, *J. Phys. Soc. Jpn.* **2005**, *74*, 1508–1520; c) J. Nishijo, A. Miyazaki, T. Enoki, *Inorg. Chem.* **2005**, *44*, 2493–2506; d) T. Enoki, K. Okabe, A. Miyazaki, in *Multifunctional Conducting Molecular Materials* (Eds.: G. Saito, F. Wudl, R. C. Haddon, K. Tanigaki, T. Enoki, H. E. Katz, M. Maesato), RSC Publishing, Cambridge, **2007**, pp. 153–160; e) A. Miyazaki, H. Yamazaki, M. Aimatsu, T. Enoki, R. Watanabe, E. Ogura, Y. Kuwatani, M. Iyoda, *Inorg. Chem.* **2007**, *46*, 3353–3366.

[6] T. Shirahata, M. Kibune, M. Maesato, T. Kawashima, G. Saito, T. Imakubo, *J. Mater. Chem.* **2006**, *16*, 3381–3390.

[7] a) M. Maesato, T. Kawashima, Y. Furushima, G. Saito, H. Kitagawa, T. Shirahata, M. Kibune, T. Imakubo, *J. Am. Chem. Soc.* **2012**, *134*, 17452–17455; b) M. Maesato, T. Kawashima, G. Saito, T. Shirahata, M. Kibune, T. Imakubo, *Phys. Rev. B* **2013**, *87*, 085117.

[8] M. Maesato, Y. Furushima, G. Saito, H. Kitagawa, T. Imakubo, A. Kiswandhi, D. Graf, J. S. Brooks, *J. Phys. Soc. Jpn.* **2013**, *82*, 043704.

[9] An iodine bond is the strongest halogen bond; a) T. Imakubo, H. Sawa, R. Kato, *Synth. Met.* **1995**, *73*, 117–122; b) T. Imakubo, N. Tajima, M. Tamura, R. Kato, Y. Nishio, K. Kajita, *J. Mater. Chem.* **2002**, *12*, 159–161; c) M. Fourmigué, P. Batail, *Chem. Rev.* **2004**, *104*, 5379–5418; d) P. Metrangolo, F. Meyer, T. Pilati, G. Resnati, G. Terraneo, *Angew. Chem. Int. Ed.* **2008**, *47*, 6114–6127; *Angew. Chem.* **2008**, *120*, 6206–6220; e) P. Politzer, J. S. Murray, *ChemPhysChem* **2013**, *14*, 278–294; f) T. Imakubo, M. Kobayashi, *Eur. J. Inorg. Chem.* **2014**, *2014*, 3973–3981.

[10] a) T. Imakubo, T. Shirahata, *Chem. Commun.* **2003**, 1940–1941; b) T. Imakubo, T. Shirahata, M. Kibune, H. Yoshino, *Eur. J. Inorg. Chem.* **2007**, 4727–4735.

[11] B. R. McGarvey, M. J. Taylor, D. G. Tuck, *Inorg. Chem.* **1981**, *20*, 2010–2013.

[12] CCDC 1054133 [**1**] and 1054132 [**2**] contain the supplementary crystallographic data for this paper. These data can be obtained free of charge from The Cambridge Crystallographic Data Centre.

[13] C. Michioka, Y. Itoh, K. Yoshimura, T. Furushima, M. Maesato, G. Saito, T. Shirahata, M. Kibune, T. Imakubo, *J. Phys. Conf. Ser.* **2009**, *150*, 042124.

[14] M. Enomoto, A. Miyazaki, T. Enoki, *Mol. Cryst. Liq. Cryst.* **1999**, *335*, 293–302.

[15] a) B. Zhang, Z. Wang, Y. Zhang, K. Takahashi, Y. Okano, H.-B. Cui, H. Kobayashi, K. Inoue, M. Kurmoo, F. L. Pratt, D. Zhu, *Inorg. Chem.* **2006**, *45*, 3275–3280; b) T. Hayashi, X. Xiao, H. Fujiwara, T. Sugimoto, H. Nakazumi, S. Noguchi, H. Aruga-Katori, *Inorg. Chem.* **2007**, *46*, 8478–8480.

[16] a) A. Paduan-Filho, C. C. Becerra, F. Palacio, *Phys. Rev. B* **1991**, *43*, 11107–11111; b) C. C. Becerra, A. Paduan-Filho, F. Palacio, V. B. Barbeta, *J. Appl. Phys.* **1993**, *73*, 5491–5493.

[17] a) G. Grüner, *Rev. Mod. Phys.* **1988**, *60*, 1129–1181; b) P. Monceau, *Adv. Phys.* **2012**, *61*, 325–581.

Received: April 27, 2015
Published online: July 14, 2015

